Karadeniz Fen Bilimleri Dergisi
The Black Sea Journal of Sciences
DOI: 10.31466/kfbd.1779548
ISSN (Online): 2564-7377
https://dergipark.org.tr/tr/pub/kfbd
Research Article / Araştırma Makalesi

Investigation of the Structural, Electronic and Biological Properties of (E)-4-(((3-(1H-benzo[d]imidazol-2-yl)phenyl)imino)methyl)benzene-1,3-diol Compound at Theoretical and Molecular Levels

(E)-4-(((3-(1H-benzo[d]imidazol-2-il)fenil)imino)metil)benzen-1,3-diol Bileşiğinin Yapısal, Elektronik ve Biyolojik Özelliklerinin Teorik ve Moleküler Düzeylerde İncelenmesi

Barış KARTAL[1]*

Abstract

In this study, the structural, electronic, and biological properties of the Schiff base derivative (E)-4-(((3-(1H-benzo[d]imidazol-2-yl)phenyl)imino)methyl)benzene-1,3-diol (BIMSB) were investigated in detail using theoretical methods. Quantum chemical calculations were performed at the B3LYP/6-31G(d,p) and B3PW91/6-31G(d,p) levels using DFT. The optimized geometry of the molecule was evaluated using electrostatic potential (MEP) maps, and reactive sites were identified. Chemical stability and reactivity analyses were performed by calculating the HOMO-LUMO energy levels and the band gap between them. Intramolecular interactions were investigated using the Natural Bonding Orbital (NBO) method, demonstrating the contribution of hyperconjugative interactions to structural stability. Furthermore, the Mulliken charge distribution was analyzed to identify electrophilic and nucleophilic centers. The molecule's nonlinear optical (NLO) properties were evaluated using dipole moment, polarizability, and hyperpolarizability parameters, demonstrating the potential of BIMSB in NLO applications. Potential biological interactions of the compound with acetylcholinesterase (AChE) enzymes (PDB: 4B84 and 4EY7) were investigated using molecular docking, and it was determined that it exhibited high binding affinities (-8.56 and -8.57 kcal/mol) with both enzymes. Finally, ADMET analyses performed using Admetlab 2.0 revealed that the compound has pharmacokinetics and potential for drug development. All the data obtained indicate that BIMSB is a promising candidate molecule for pharmaceutical and technological applications.

Keywords: Schiff base, DFT, MEP, NBO, Molecular Docking, ADMET.

Öz

Bu çalışmada, Schiff bazı türevi olan (E)-4-(((3-(1H-benzo[d]imidazol-2-yl)phenyl)imino)methyl)benzene-1,3-diol (BIMSB) bileşiğinin yapısal, elektronik ve biyolojik özellikleri teorik yöntemlerle detaylı olarak incelenmiştir. Kuantum kimyasal hesaplamalar, DFT kapsamında B3LYP/6-31G(d,p) ve B3PW91/6-31G(d,p) düzeylerinde gerçekleştirilmiş; molekülün optimize geometrisi, elektrostatik potansiyel (MEP) haritaları ile değerlendirilmiş ve reaktif bölgeler belirlenmiştir. HOMO-LUMO enerji seviyeleri ve aralarındaki bant aralığı hesaplanarak kimyasal kararlılık ve reaktivite analizi yapılmıştır. Molekül içi etkileşimler Doğal Bağ Orbitalü (NBO) yöntemiyle incelenmiş; hiperconjugatif etkileşimlerin yapısal stabiliteye katkısı gösterilmiştir. Ayrıca Mulliken yük dağılımı, elektrofilik ve nükleofilik merkezleri belirlemek amacıyla analiz edilmiştir. Molekülün doğrusal olmayan optik (NLO) özellikleri; dipol moment, polarizabilite ve hiperpolarizabilite parametreleri üzerinden değerlendirilmiş ve BIMSB'nin NLO uygulamalarında potansiyel taşıdığı ortaya konmuştur. Bileşiğin asetilkolinesteraz (AChE) enzimleri (PDB: 4B84 ve 4EY7) ile olası biyolojik etkileşimleri moleküler doking yöntemiyle araştırılmış ve her iki enzimle de yüksek bağlanma afinitesi (-8.56 ve -8.57 kcal/mol) sergilediği belirlenmiştir. Son olarak, Admetlab 2.0 aracı ile yapılan ADMET analizleri sonucunda bileşiğin farmakokinetik açıdan uygun ve ilaç geliştirme potansiyeli taşıdığı saptanmıştır. Elde edilen tüm veriler, BIMSB'nin farmasötik ve teknolojik uygulamalarda değerlendirilmesi açısından umut vadeden bir molekül adayı olduğunu göstermektedir.

Anahtar Kelimeler: Schiff bazı, DFT, MEP, NBO, Moleküler Doking, ADMET.

[1]Adıyaman University, Gölbaşı Vocational School, Property Protection and Security Department, Adıyaman, Türkiye

***Corresponding Author/Sorumlu Yazar:** baris.j.kartal@gmail.com

Received/Geliş: 07.09.2025 **Accepted/Kabul:** 20.04.2026 **Published/Yayın:** 17.08.2026

Kartal, B. (2026). Investigation of the Structural, Electronic and Biological Properties of (E)-4-(((3-(1H-benzo[d]imidazol-2-yl)phenyl)imino)methyl)benzene-1,3-diol Compound at Theoretical and Molecular Levels. *Karadeniz Fen Bilimleri Dergisi*, 16(3), 1047-1067. https://doi.org/10.31466/kfbd.1779548

1. Introduction

Alzheimer's disease (AD) is a neurodegenerative disorder characterized by cognitive impairment and memory loss, with dysfunction of the cholinergic system playing a significant role in its pathogenesis (Peitzika & Pontiki, 2023). Acetylcholinesterase (AChE), the primary enzyme that rapidly hydrolyzes acetylcholine in the synaptic cleft, is a critical factor in the reduction of cholinergic transmission in AD. Literature has shown that AChE is involved not only in acetylcholine metabolism but also interacts with beta-amyloid (Aβ) plaques, promoting amyloid deposition, which is highlighted as a secondary mechanism in the pathophysiology of the disease (Farihi et al., 2023). Treatment with AChE inhibitors (AChEIs) is known to temporarily improve cognitive performance and slow disease progression to a limited extent by increasing synaptic acetylcholine levels. However, the efficacy of current AChEIs is limited, and they do not show a significant long-term effect on the core pathological processes of the disease. Current research focuses on the development of inhibitors with multi-effect potential targeting different isoforms of AChE and their interaction mechanisms with amyloid plaques, thereby enabling simultaneous intervention in both cholinergic deficiency and amyloid toxicity (Araújo et al., 2011).

Schiff bases are compounds formed by the condensation of primary amines with carbonyl groups and contain the characteristic azomethine (C=N) functional group (Salihović et al., 2021). These molecules have broad biomedical potential due to both their flexibility in chemical structure and their strong coordination abilities with metal ions. In particular, the demonstration of the targeted biological activities of Schiff bases in complex diseases such as Alzheimer's disease has created a significant research area for modern drug design (Gul et al., 2024). In this context, theoretical chemistry and computational methods guide experimental studies by providing detailed analysis of the electronic structures of molecules. Density Functional Theory (DFT) calculations provide critical data for understanding biological activity by revealing the geometric optimizations, energy levels, molecular orbitals, and electronic distributions of molecules. DFT methods enable precise modeling of the electronic properties of molecules, particularly using hybrid functionals such as B3LYP and B3PW91(Babu et al., 2011).

In addition, molecular docking studies are a powerful tool for examining the interaction mechanisms between target proteins and ligands at the atomic level, calculating molecular recognition processes and binding energies (Çimen et al., 2025). This method allows for predicting biological activity and specificity by determining how potential drug candidates interact with target biomolecules (Tahiroğlu et al., 2025). This provides preliminary information that can guide experimental studies and accelerates the drug development process (Gören, Bağlan, Tahiroğlu, et al., 2024). Additionally, ADMET (Absorption, Distribution, Metabolism, Excretion, Toxicity) analyses

are performed to predict the pharmacokinetic properties of newly developed molecules (El-Shamy et al., 2022). The ADMET profile contains critical information such as how a compound is absorbed, distributed, metabolized, and excreted in the body. These parameters are crucial for drug efficacy and safety, and their early prediction reduces the risk of clinical failure (Ahmad et al., 2023).

The pharmaceutical significance of Schiff bases has been extensively discussed in the literature. In particular, a review published by Mushtaq et al (Mushtaq et al., 2024). details the synthesis mechanisms and biological activities of Schiff bases, including antibacterial, antifungal, antiviral, and antioxidant properties. This study evaluated the general structural characteristics and biological potential of Schiff bases based on examples from the literature; however, it did not include detailed quantum chemical and computational biology analyses for specific molecules. The molecule (E)-4-(((3-(1H-benzo[d]imidazol-2-yl)phenyl)imino)methyl)benzene-1,3-diol (BIMSB) (Mushtaq et al., 2024) examined in this study belongs to the class of Schiff base compounds outlined in Mushtaq et al.'s review article; however, the mentioned above article did not report any theoretical or computational analyses of the structural, electronic, NLO, and biological properties of this molecule. Therefore, while the current study is inspired by the mentioned above review article in terms of molecule selection, it presents a completely original investigation in terms of methodology, scope, and scientific objectives. The unique aspect of this study is the detailed electronic structure analysis of the BIMSB molecule using two different DFT functionals (B3LYP and B3PW91), the simultaneous evaluation of advanced quantum chemical parameters such as MEP, HOMO–LUMO, NBO, and Mulliken charge distribution, and the first-ever reporting of its nonlinear optical (NLO) properties. Furthermore, while biological activity is generally discussed in the literature based on experimental results, this study integrates molecular docking analyses performed with AChE enzymes (PDB: 4B84 and 4EY7) and ADMET predictions to evaluate the molecule as a potential drug candidate. In conclusion, while the study by Mushtaq et al. provides a general framework regarding the pharmaceutical importance of Schiff bases, the present study offers a unique and complementary contribution to the literature by presenting the multifaceted theoretical characterization of a specific Schiff base derivative and its interaction with biological targets.

2. Materials and Methods

The investigated compound was first designed in two-dimensional (2D) form using ChemBioDraw Ultra software. The three-dimensional (3D) conformer of the designed structure was created using Chem3D Pro, and initial energy minimization was performed. The minimized structure obtained was imported into Gaussian 09 (G.W.T. M.J. Frisch, 2009) software for quantum chemical calculations. Structural optimization was performed in the gas phase using the density functional

theory (DFT) approach. Calculations were performed using B3LYP, B3PW91 methods, and the 6-31G(d) basis set. Absorption, distribution, metabolism, and excretion (ADMET) parameters, which are critical in the drug development process, were analyzed using the online tool Admetlab 2.0 (https://admetmesh.scbdd.com) to evaluate the pharmacokinetic suitability of the compound. Parameters such as Lipinski's rules, bioavailability, gastrointestinal absorption, and blood-brain barrier permeability were taken into account in these analyses. Molecular docking studies were conducted to investigate the interactions of the compound with the biological target. To investigate ligand-enzyme interactions and evaluate the binding potential of the compound to the target protein as an enzyme inhibitor, molecular docking studies were performed using the Schrödinger Maestro Molecular Modeling platform (version 11.8) (Release, 2019). In this context, the target protein structure was obtained from the Protein Data Bank (PDB) (Burley et al., 2019). The best docking positions were visualized in 2D and 3D formats using Discovery Studio 2021 Client software (Systèmes, 2016).

3. Results and Discussion

3.1. Structure Details and Analysis

Bond lengths and bond angles are the main determinants in understanding the geometric structures of molecules (Gören, Bağlan, et al., 2024a). These parameters vary depending on factors such as the bond character between atoms within the molecule, the hybridization state, and the electron density distribution. Quantum chemical calculations, in particular, can predict bond lengths and bond angles with high accuracy (Tahiroğlu, Gören, Bağlan, et al., 2024). In this study, the optimized geometric structure of the (BIMSB) molecule (Figure 1) was obtained using the B3LYP and B3PW91 methods and the 6-31G(d,p) basis set within the scope of density functional theory (DFT). A high level of agreement was observed between the bond lengths and bond angles calculated by both methods (Table 1). The bond lengths and bond angles obtained by both methods provide important information about the overall structural stability and planarity of the molecule. C–C bond lengths within the aromatic rings were found to be in the range of 1.39–1.40 Å on average in both methods, indicating that the aromatic character is preserved. Conjugated C–N bonds, such as C1–N9 and C6–N7, have values between single and double bond character, indicating resonance and electron delocalization. The significant differences observed between the two methods, particularly in the N7–C8 and C8–N9 bonds, indicate that method sensitivity and electronic structure are influential in this region. Furthermore, while the calculated torsion angles reveal that the molecule is largely planar, the presence of partial bends in regions near the imino group is important for conformational flexibility. Theoretically obtained geometric data indicate that BIMSB is a potential inhibitor candidate that can

interact with acetylcholinesterase enzymes with high affinity. The molecule's planar structure, conjugated systems, and hydrogen-bonding functional groups are key features that contribute to the stability of the enzyme-ligand complex. Based on these findings, molecular docking studies are recommended to investigate the binding behavior of BIMSB with AChE enzymes in detail.

Table 1. Theoretically obtained some bond lengths (Å) and bond angles (°) of the BIMSB molecule.

Bond Lengths	B3LYP	B3PW91	Bond Angles	B3LYP	B3PW91
C1-C2	1.40143	1.39976	C1-C2-C3	118.03491	118.00602
C2-C3	1.39036	1.38817	C2-C3-C4	121.43604	121.46729
C5-C6	1.39564	1.39399	C3-C4-C5	121.55675	121.59285
C1-C6	1.42761	1.41523	C1-C6-C5	122.59085	122.64631
C1-N9	1.38322	1.37859	C1-N9-C8	105.49659	105.34796
C6-N7	1.38258	1.37773	C1-C6-N7	104.46961	104.41321
N7-C8	1.38522	1.31524	N7-C8-N9	107.32973	112.42633
C8-N9	1.31733	1.46437	C10-C8-N7	124.69754	123.00752
C8-C10	1.46725	1.46437	N9-C8-C10	124.69754	124.56613
C10-C15	1.40412	1.40171	C10-C15-C14	119.91424	124.56613
C10-C11	1.40200	1.39967	C22-C21-O25	122.18251	122.19035
C15-C14	1.39232	1.39045	C19-C20-C21	121.17255	121.04181
C14-C13	1.39317	1.39121	C12-N16-C17	123.08859	121.04181
C13-C12	1.40332	1.40133	N16-C17-C18	122.34495	122.04144
C12-C11	1.40301	1.40133	C18-C23-O24	121.67637	121.50354
C17-C18	1.44207	1.43800	Planar Bond Angles	B3LYP	B3PW91
C18-C19	1.41084	1.40846	C3-C2-C1-N9	179.56186	179.56010
C18-C23	1.42631	1.42456	C4-C3-C6-N7	179.70917	179.73673
C23-O24	1.33742	1.33081	C1-N9-C8-C10	179.62062	179.63994
C23-C22	1.39373	1.39815	N7-C8-C10-C15	164.90332	163.80839
C22-C21	1.08115	1.39208	C8-C10-C15-C14	-178.29950	-178.25901
C21-C20	1.40855	1.40728	C13-C12-N16-C17	143.72059	142.91070
C20-C19	1.38061	1.37841	C19-C18-C23-O24	-179.64821	-179.60979

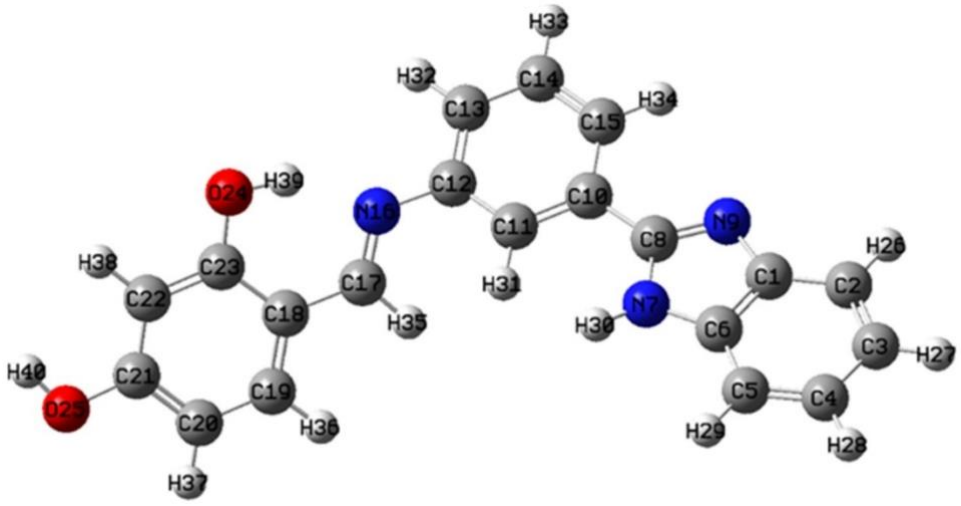

Figure 1. Optimized geometry representation of BIMSB compound by B3LYP method.

3.2. Mulliken Atomic Charges

Mulliken atomic charge is a fundamental quantum chemical approach used to determine the electronic charge distribution of atoms in molecules (Gören, Bağlan, et al., 2025b; Tahiroğlu, Gören, Çimen, et al., 2024) . In this method, the electron density contributing to each atom's atomic orbital is directly assigned to that atom, while the electron density resulting from the overlap between the orbitals of two or more atoms is equally distributed among the atoms involved (Khosravi et al., 2020). Mulliken charges are one of the important parameters that directly affect the electronic structure, polarizability, dipole moment, and chemical reactivity of a molecule (Gören, Bağlan, et al., 2024b). The Mulliken atomic charge distributions for the BIMSB molecule were calculated using the B3LYP and B3PW91 methods within the framework of density functional theory (DFT), and the results have been presented in Table 2. The results obtained by both methods are generally consistent and provide important information about the electron densities of the atoms in the molecule. First, nitrogen atoms (N7, N9, N16), which constitute fundamental structural units of the molecule, were observed to carry a negative charge in both calculation methods. This suggests that nitrogen atoms, due to their high electronegativity, tend to attract electron density. In particular, the N7 atom is among the most negatively charged atoms in the molecule, with a Mulliken charge of -0.618 in the B3LYP method and -0.641 in B3PW91. Oxygen atoms (O22, O24, and O25) also carry a similarly high negative charge, indicating increased electron density and a high potential for hydrogen bonding. The most striking value belongs to the O25 atom, carrying a charge of -0.570 (B3LYP) and -0.580 (B3PW91). A significant difference in charge distribution was observed between the carbon atoms due to differences in their local electronic environments. The C8 (0.373/0.392) and C23 (0.280/0.286) atoms carry positive charges, indicating an electron deficiency in these regions. In contrast, carbons such as C3 (-0.105/-0.143), C4 (-0.104/-0.140), and C19 (-0.169/-0.192) carry negative charges, reflecting different hybridization states and bond structures. Hydrogen atoms generally have low positive charge values (H26: 0.104/0.142) and exhibit partial positive character depending on the electron configuration of the atoms to which they are bonded. However, the higher positive charge of H30 (0.284/0.303) compared to other hydrogens may be due to the electronic structure of the group to which it is bonded, and this should be taken into account in the analysis of intramolecular weak interactions. When the Mulliken charge distribution of the molecule is examined, it is observed that nitrogen (N7, N9, N16) and oxygen (O22, O24, O25) atoms in particular have high negative charge values. These atoms can exert their inhibitory effects by forming hydrogen bonds or electrostatic interactions with positively charged amino acid residues in the active site of AChE. The high negative charges of O24 and O25 (in the range of -0.555 to -0.580) in particular can serve as critical binding sites for the molecule to bind to the enzyme. These oxygen atoms can stabilize the inhibitor's binding by forming strong hydrogen bonds with serine or histidine residues in the enzyme. The negative

charges of the nitrogen atoms facilitate electrostatic attraction with positive sites on the enzyme surface. Positively charged carbons (C8 and C21) and hydrogens (H30) contribute to the molecule's structural stability and may contribute to hydrophobic or van der Waals interactions during binding with the enzyme.

Table 2. Mulliken atomic charges of the BIMSB molecule.

ATOMS	B3LYP	B3PW91	ATOMS	B3LYP	B3PW91
C1	0.213	0.213	C21	0.320	0.316
C2	-0.099	-0.114	O22	-0.145	-0.182
C3	-0.105	-0.143	C23	0.280	0.286
C4	-0.104	-0.140	O24	-0.555	-0.566
N7	-0.618	-0.641	O25	-0.570	-0.580
C8	0.373	0.392	H26	0.104	0.142
N9	-0.514	-0.529	H27	0.093	0.130
C10	0.064	0.031	H28	0.094	0.130
C11	-0.152	-0.170	H29	0.097	0.135
C12	0.244	0.232	H30	0.284	0.303
C13	-0.111	-0.141	H31	0.102	0.136
C14	-0.097	-0.136	H32	0.104	0.142
C15	-0.086	-0.106	H33	0.098	0.135
N16	-0.473	-0.483	H34	0.117	0.153
C17	0.117	0.113	H35	0.083	0.111
C18	0.090	0.051	H36	0.100	0.135
C19	-0.169	-0.192	H37	0.102	0.140
C20	-0.120	-0.158	H38	0.095	0.133

3.3. HOMO and LUMO Analysis

The most important parameters in determining the chemical reactivity of molecules are the frontier orbitals, called HOMO (Highest Occupied Molecular Orbital) and LUMO (Lowest Unoccupied Molecular Orbital) (Tahiroğlu, Gören, Yıldıko, et al., 2024). The difference between the HOMO and LUMO energies, i.e., the HOMO-LUMO gap, directly affects the chemical stability, reactivity, hardness, and softness of a molecule (Gören, Bağlan, et al., 2025a; Jayaprakash et al., 2011) . As this gap decreases, the molecule more easily participates in electron transfer processes, thereby increasing its chemical reactivity. Therefore, a lower HOMO-LUMO energy gap indicates that the molecule is less stable but exhibits higher reactivity. These properties are critical for understanding the reaction mechanisms of molecules and for designing new chemical compounds (Karabacak et al., 2015). Figure 2 and Figure 3 show the frontier molecular orbitals of the (BIMSB) molecule at two different levels, B3LYP and B3PW91. The electronic properties of the BIMSB compound were calculated using the B3LYP and B3PW91 methods within the DFT framework, using the optimized geometry with the 6-31G(d,p) basis set. The obtained frontier molecular orbital (FMO) energies and global reactivity descriptors provide important information about the chemical stability

and reactivity of the compound (Table 3). The HOMO and LUMO energy levels play a critical role in determining the tendency of the molecule to undergo bond-making and bond-breaking processes. For the BIMSB compound, the HOMO energy was calculated as –6.4649 eV and the LUMO energy as –0.4094 eV according to the B3LYP method. Similarly, according to the B3PW91 method, these values were –6.4070 eV (EHOMO) and –0.3840 eV (ELUMO), respectively. 0.1650to occur. Indeed, the calculated energy range (ΔE=|EHOMO−ELUMO|) is 6.0555 eV for B3LYP and 6.0230 eV for B3PW91, indicating that the compound has a very stable chemical structure. The ionization potential (I=–EHOMO) and electron affinity (A=–ELUMO) values were found to be 6.4649 eV and 0.4094 eV (B3LYP); 6.4070 eV and 0.3840 eV (B3PW91), respectively. These values quantitatively express the molecule's resistance to losing an electron and its tendency to gain an electron. In addition, chemical hardness (η), chemical softness (s), chemical potential (μ), electronegativity (χ), and electrophilicity index (ω) were calculated from the global reactivity descriptors. Chemical hardness values were obtained as 3.0278 eV and 3.0115 eV for the B3LYP and B3PW91 methods, respectively. Low softness values (s=0.1650 and 0.1660) indicate a high degree of rigidity in the electron cloud of the molecule and a low nucleophilic tendency. Chemical potential (μ) values were –3.4372 eV (B3LYP) and –3.3955 eV (B3PW91), indicating the molecule's tendency to accept electrons. Electronegativity (χ) values calculated from these values were 3.4372 eV and 3.3955 eV, respectively. Electrophilicity index (ω), i.e., the electrophilic character of the molecule, was determined as 1.9515 eV (B3LYP) and 1.9143 eV (B3PW91). These values indicate that BIMSB has moderate electrophilic character. Overall, the obtained data reveal that BIMSB has high chemical stability and low reactivity.

Table 3. HOMO and LUMO energy values calculated for the BIMSB molecule by the B3LYP and B3PW91 methods.

Molecules Energy		B3LYP	B3PW91
E_{LUMO}		-0.4094	-0.3840
E_{HOMO}		-6.4649	-6.4070
E_{LUMO+1}		-0.4857	-0.4441
E_{HOMO-1}		-6.8010	-6.7560
Energy Gap	$(\Delta E)\lvert E_{HOMO}-E_{LUMO}\rvert$	6.0555	6.0230
Ionization Potential	$(I=-E_{HOMO})$	6.4649	6.4070
Electron Affinity	$(A=-E_{LUMO})$	0.4094	0.3840
Chemical hardness	$(\eta=(I-A)/2)$	3.0278	3.0115
Chemical softness	$(s=1/2\eta)$	0.1650	0.1660
Chemical Potential	$(\mu=-(I+A)/2)$	-3.4372	-3.3955
Electronegativity	$(\chi=(I+A)/2)$	3.4372	3.3955
Electrophilicity index	$(\omega=\mu^2/2\eta)$	1.9515	1.9143

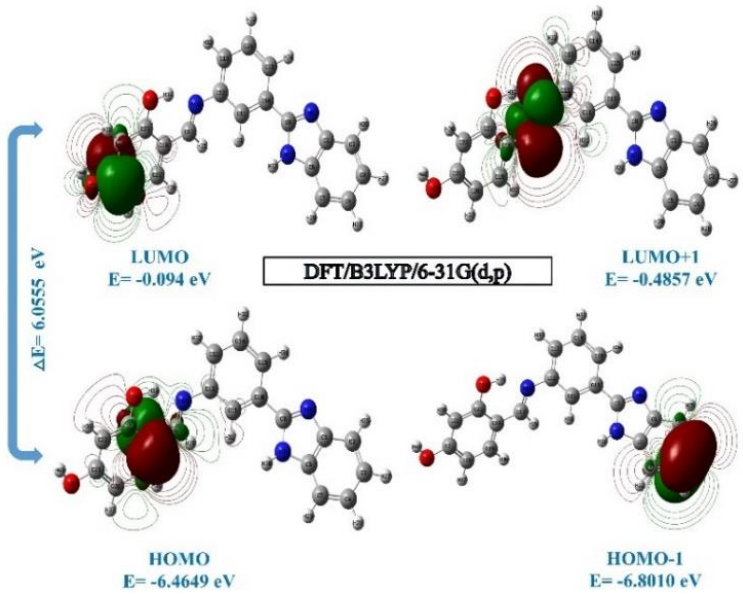

Figure 2. Boundary molecular orbitals of the BIMSB molecule according to the B3LYP method.

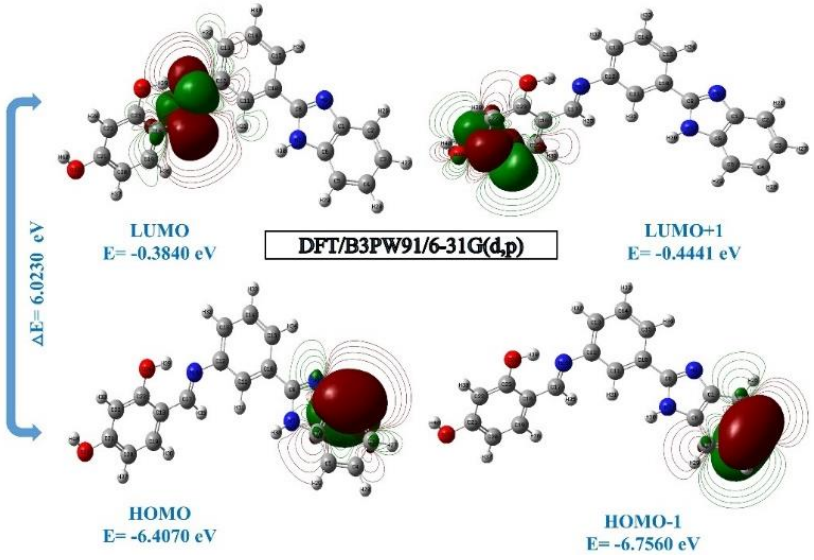

Figure 3. Boundary molecular orbitals of the BIMSB molecule according to the B3PW91 method.

3.4. Molecular Electrostatic Potential (MEP)

The molecular electrostatic potential (MEP) surface is used as an important tool for understanding the electronic properties of a molecule by visualizing the three-dimensional distribution of electrostatic potential (Gören, Bağlan, & Yıldıko, 2025). MEP surfaces are directly related to the molecule's dipole moment, electronegativity differences, and partial charge distribution between atoms (Ganiev et al., 2023). This analysis method is frequently used for determining electrophilic and nucleophilic reaction sites, as well as for identifying hydrogen bonding interactions. Figure 4 presents the molecular electrostatic potential (MEP) surfaces obtained for the BIMSB molecule using the B3LYP and B3PW91 methods. In the MEP maps, red colors represent the negative

electrostatic potential, indicating regions with high electron density. These regions are theoretically considered attractive centers for electrophilic species. In contrast, the positive electrostatic potential regions shown in blue correspond to areas with low electron density and represent suitable interaction sites for nucleophilic species. In the BIMSB molecule, the negative electrostatic potential is observed to be concentrated particularly around the nitrogen atoms in the benzimidazole ring and the phenolic hydroxyl and imine groups. This suggests that these functional groups may play a role in electrophilic interactions and as hydrogen bond acceptors. The positive electrostatic potential, on the other hand, is predominantly localized around aromatic and aliphatic hydrogen atoms, indicating that these regions are more susceptible to interaction with nucleophilic species. The compatibility of the MEP surfaces calculated using the B3LYP and B3PW91 methods indicates that the electrostatic potential distribution exhibits a similar trend regardless of the method, which supports the reliability of the theoretical calculations. Furthermore, the variation of electrostatic potential values between approximately −7 a.u. and +7 a.u. reveals that the BIMSB molecule has a stable charge distribution.

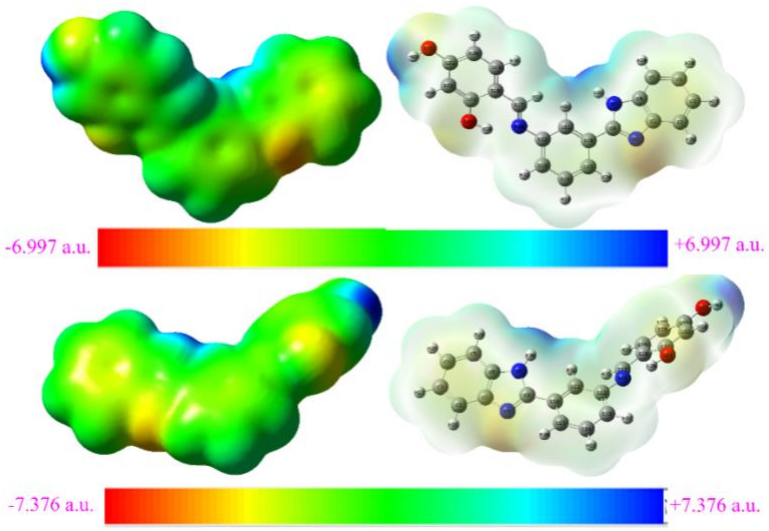

Figure 4. Molecular electrostatic potential surface of the BIMSB molecule using B3LYP and B3PW91 methods.

3.5. Non-Linear Optical Properties (NLO)

Nonlinear optical (NLO) materials are indispensable components of emerging technologies such as telecommunications and signal processing due to their fundamental functions, particularly in areas such as frequency shifting, optical modulation, switching, laser systems, fiber optic technologies, optical materials engineering, and optical memory (Gören & Yıldıko, 2024). The increasing demand for NLO materials requires a more in-depth understanding of the relationship between their electronic structure and NLO response (Moustafa et al., 2020). The dipole moment (Debye), polarizability (α, au), and hyperpolarizability (β, esu) components of the BIMSB molecule

were calculated using the B3LYP, B3PW91, and 6-31G(d) basis set methods within the framework of density functional theory (DFT), and the results have been presented in Table 4. The NLO-based quantum chemical properties were calculated using Equations 1-4. Fundamental molecular properties such as dipole moment, polarizability, and first hyperpolarizability (β) provide crucial information about the electronic structure of the compound. According to the results, the total dipole moment of BIMSB was calculated as 2.2943 Debye by the B3LYP method and 2.3337 Debye by the B3PW91 method. These values indicate that the molecule has a moderately polar structure and is sensitive to electrostatic interactions. The average polarizability (⟨α⟩) was obtained as 132.64 and 131.08 a.u., respectively, indicating that the molecule has a significant deformation ability against external electric fields. The nonlinear optical (NLO) reactions of BIMSB were evaluated in comparison with urea, a widely used reference compound. As a result of the calculations, the total first hyperpolarizability (β) value of BIMSB was obtained as 1.171×10^{-30} esu by the B3LYP method and 1.086×10^{-30} esu by the B3PW91 method. These values indicate that the experimentally reported β value of approximately 0.3728×10^{-30} esu for urea is approximately three times lower than the BIMSB values calculated by both methods. In this context, BIMSB exhibits a much higher nonlinear optical response compared to urea and can be considered as a potential NLO material. Furthermore, the dipole moment of BIMSB (approximately 2.3 Debye) is significantly higher than the dipole moment of urea, which is around 1.5 Debye, indicating that the molecule has a stronger electrostatic interaction potential under external electric fields.

$$\mu = \left(\mu_x^2 + \mu_y^2 + \mu_z^2\right)^{1/2} \quad (1)$$

$$\alpha_{\text{Total}} = \frac{1}{3}(\alpha_{xx} + \alpha_{YY} + \alpha_{zz}) \quad (2)$$

$$\beta_{Total} = (\beta^2 x + \beta^2 y + \beta^2 z)^{1/2} \quad (3)$$

$$= [(\beta xxx + \beta xyy + \beta xzz)^2 + (\beta yyy + \beta yxx + yzz)^2 + (\beta zzz + \beta zxx + \beta zyy)^2]^{\frac{1}{2}} \quad (4)$$

Table 4. The dipole moments (Debye), polarizability (au), components, and total value of the BIMSB molecule calculated by B3LYP and B3PW91 methods.

Parameters	B3LYP	B3PW91	Parameters	B3LYP	B3PW91
β_{XXX}	-128.3461	-120.6816	μ_x	-0.9619	-0.9173
β_{YYY}	21.9442	22.4396	μ_y	-1.3881	-1.4016
β_{ZZZ}	5.9436	5.5799	μ_z	1.5529	1.6248
β_{XYY}	25.2817	27.9513	$\mu_{(D)}$	2.2943	2.3337
β_{XXY}	5.9156	4.3979	αxx	-122.0669	-118.7247
β_{XXZ}	-45.7217	-41.2492	α_{YY}	-130.8022	-128.8776
β_{XZZ}	-24.1716	-25.5297	αzz	-145.0476	-145.6328
β_{YZZ}	-2.3919	-1.6947	α_{XY}	-12.0179	-12.1807
β_{YYZ}	0.5148	0.6814	α_{XZ}	1.6994	1.9636
β_{XYZ}	-24.7180	-24.2907	α_{YZ}	2.5699	2.8007
β(esu)	1.171×10^{-30}	1.086×10^{-30}	α(au)	132.6389	131.0784

3.6. NBO Analysis

NBO analysis is a powerful method that allows for the detailed investigation of intermolecular and intramolecular bonds. This analysis is particularly important for understanding processes such as charge transfer and conjugative (resonance-based) interactions (Sakr et al., 2022). NBO analysis of the BIMSB compound at the B3LYP/6-31G(d,p) level provides detailed insights into the electron delocalization and stabilization mechanisms of the molecule (Table 5). The analyses show that the occupancy of the σ bonds is in the range of 1.971–1.984 e and that of the π bonds is in the range of 1.764–1.985 e, which confirms that the molecule possesses strong covalent bonds and efficient electron delocalization in aromatic-conjugated systems. When donor-acceptor interactions are examined, the high stabilization energies of the π→π* interactions are particularly noteworthy; The C10–C11 π→C8–N9π* interaction provides strong conjugative stabilization with a value of 15.39 kcal/mol, the N16–C17 π→C12–C13π* interaction with 12.25 kcal/mol, and the C8–N9π→C1–C6π* interaction with 12.01 kcal/mol. Additionally, the C1–C6 π→C4–C5π* (10.29 kcal/mol) and C2–C3 π→C4–C5π* (10.52 kcal/mol) interactions support effective electron delocalization between the aromatic rings of the molecule. Hyperconjugative interactions of σ→σ* also make significant contributions, with interactions such as C2–H26 σ→C3–C4 σ* (4.70 kcal/mol), C5–H29 σ→C3–C4 σ* (4.58 kcal/mol), and C19–H36 σ→C18–C23 σ* (5.71 kcal/mol), strengthening the structural stability of the molecule. The role of heteroatoms cannot be ignored; nitrogen-containing groups such as C8–N9 and N16–C17 interact with both π and π* orbitals, facilitating intrinsic electron transfer and thereby enhancing the electronic and optical properties of the molecule. The Fock matrix elements (0.049–0.066 a.u.) and energy differences (0.28–0.37 a.u.) confirm the strong overlap between donor and acceptor orbitals. Overall, NBO analysis shows that BIMSB possesses high stability through both conjugative and hyperconjugative interactions, and that heteroatom contributions and effective charge delocalization enhance the molecule's electronic potential.

Table 5. Selected NBO results of the BIMSB molecule calculated by B3LYP method.

NBO(i)	Type	Occupancies	NBO(j)	Type	Occupancies	E(2)[a] (Kcal/mol)	E (j)-E(i)[b] (a.u.)	F (i, j)[c] (a.u)
C1-C2	σ	1.97650	C6-N7	σ*	1.98140	3.20	0.98	0.050
C1-C6	π	1.98111	C4-C5	π*	1.83247	10.29	0.31	0.051
C1-N9	σ	1.97116	C8-C10	σ*	1.97658	7.02	1.09	0.078
C2-C3	π	1.83359	C4-C5	π*	1.83247	10.52	0.30	0.050
C2-H26	σ	1.98287	C3-C4	σ*	1.98067	4.70	0.92	0.059
C3-C4	σ	1.98067	C5-H29	σ*	1.98345	3.04	1.09	0.052
C3-H27	σ	1.98405	C1-C2	σ*	1.97650	4.68	0.95	0.060
C4-C5	π	1.83247	C1-C6	π*	1.98111	10.68	0.32	0.054
C4-H28	σ	1.98376	C5-C6	σ*	1.97541	4.79	0.94	0.060
C5-C6	σ	1.97541	C1-C6	σ*	1.98111	3.41	1.30	0.059
C5-H29	σ	1.98345	C3-C4	σ*	1.98067	4.58	0.92	0.058
N7-H30	σ	1.95071	C8-N9	σ*	1.89339	4.59	0.65	0.051
C8-N9	π	1.89339	C1-C6	π*	1.98111	12.01	0.37	0.062
C8-C10	σ	1.97658	C11-C12	σ*	1.97645	3.21	1.04	0.052
C10-C11	π	1.78898	C8-N9	π*	1.89339	15.39	0.28	0.059

C10-C15	σ	1.97338	N7-C8	σ*	1.98646	2.84	0.93	0.046
C11-C12	σ	1.97645	C8-C10	σ*	1.97658	4.57	1.01	0.061
C11-H31	σ	1.97764	C10-C15	π*	1.97338	5.35	0.94	0.063
C12-C13	π	1.76483	N16-C17	π*	1.90913	11.14	0.28	0.052
C12-N16	σ	1.97906	C17-C18	σ*	1.97403	3.92	1.11	0.059
C13-C14	σ	1.97660	C12-N16	σ*	1.97906	5.25	0.98	0.064
C13-H32	σ	1.98099	C11-C12	σ*	1.97645	5.77	0.93	0.066
C14-C15	π	1.98551	C10-C11	π*	1.78898	11.16	0.30	0.052
C14-H33	σ	1.98311	C10-C15	σ*	1.97338	5.08	0.94	0.062
C15-H34	σ	1.98199	C13-C14	σ*	1.97660	4.93	0.93	0.060
N16-C17	π	1.90913	C12-C13	π*	1.76483	12.25	0.36	0.061
C17-C18	π	1.97403	C12-N16	π*	1.97906	4.69	1.00	0.061
C18-C19	π	1.77952	N16-C17	π*	1.90913	13.88	0.29	0.058
C18-C19	π	1.77952	C22-C23	π*	1.82536	11.83	0.30	0.053
C19-C20	σ	1.97100	C21-O25	σ*	1.99396	5.50	0.88	0.062
C19-H36	σ	1.98115	C18-C23	σ*	1.97582	5.71	0.94	0.066
C20-C21	π	1.98470	C18-C19	π*	1.98137	11.77	0.31	0.054
C20-C21	π	1.98470	C22-C23	π*	1.82536	9.72	0.31	0.049
C20-H37	σ	1.98028	C21-C22	σ*	1.97546	5.32	0.92	0.063
C22-C23	π	1.82536	C20-C21	π*	1.98470	11.80	0.31	0.055
C22-H38	σ	1.97893	C18-C23	σ*	1.97582	5.28	0.94	0.063

3.7. Molecular Docking Studies

In this study, to investigate the interactions of BIMSB with various enzymes, the relevant protein crystal structures were obtained from the Protein Data Bank (Burley et al., 2019). Acetylcholinesterase (AChE), an important enzyme associated with the nervous system, was selected as the target protein, and the crystal structures of these proteins were provided under PDB IDs: 4B84 and 4EY7, respectively. Molecular docking studies were performed using the Schrödinger Maestro Molecular Modeling platform (version 11.8) (Release, 2019). Based on previous studies, the ligand BIMSB and protein preparation processes were performed using the LigPrep and Protein Preparation modules, respectively. During this preparation, missing protein atoms were added, hydrogen atoms were introduced, and elements that did not affect the binding site, such as crystal water molecules, were removed. Following docking analyses, the binding affinities of BIMSB for the enzymes with PDB IDs: 4B84 and 4EY7 were calculated as -8.56 kcal/mol and -8.57 kcal/mol, respectively. Table 6 demonstrates the compound's high binding affinity for the target enzymes. Inhibition of acetylcholinesterase (AChE), a key enzyme involved in the pathophysiology of Alzheimer’s disease, is a well-established therapeutic strategy; therefore, the strong interactions of BIMSB with this enzyme provide a relevant biomolecular basis for its potential application in Alzheimer’s disease. These results indicate that the compound exhibits similar strong binding affinity for both target enzymes. Details of the compound's molecular interactions with these enzymes have been presented in Table 7. According to the table, BIMSB compound formed Van der Waals interactions with the 4B84 enzyme via amino acids such as GLU-389, ASP-390, HIS-387, ARG-522 and GLN-413. In

addition, conventional hydrogen bonds of 5.36 Å and 6.20 Å in length were established with THR-505 and ARG-534, respectively. Pi-cation (7.56 Å) interactions with ARG-534, pi-sulfur (6.42 Å) with CYS-529 and amide-pi stacking (5.85 Å) interactions with ALA-412 were also recorded. In addition, pi-alkyl interactions (5.20 Å and 4.57 Å) were observed with ALA-526 and PRO-388; A 4.32 Å negative acceptor–acceptor interaction was detected with ALA-506. In interactions with the 4EY7 enzyme, BIMSB formed van der Waals contacts with amino acids GLU-243, PRO-290, ASN-533, GLN-413, and TRP-532. Hydrogen bonds of 4.71 Å and 6.97 Å were also formed with GLN-369 and ARG-247, respectively. Pi-alkyl interactions were observed with PRO-235 (at two different positions) and PRO-410 (4.63 Å, 4.87 Å, and 6.10 Å), pi–sigma and negative donor–donor interactions with ARG-296 (6.13 Å and 5.42 Å), and pi–pi T-shaped interactions with HIS-405 (5.75 Å). This versatile interaction profile indicates that BIMSB exhibits stable and specific binding to both enzymes and can therefore be considered as a potential enzyme inhibitor. The best docking positions were visualized in 2D and 3D formats using Discovery Studio 2021 Client software (Systèmes, 2016) (Figures 5-6). The obtained results provide important information for understanding the potential interactions of BIMSB with these enzymes and for evaluating their pharmacological properties.

Table 6. Molecular docking interactions scores with PDBID: 4B84, PDBID: 4EY7 enzymes of BIMSB compound.

Compound	Docking Score	
	(PDB: 4B84)	(PDB: 4EY7)
(BIMSB)	-8.56	-8.57

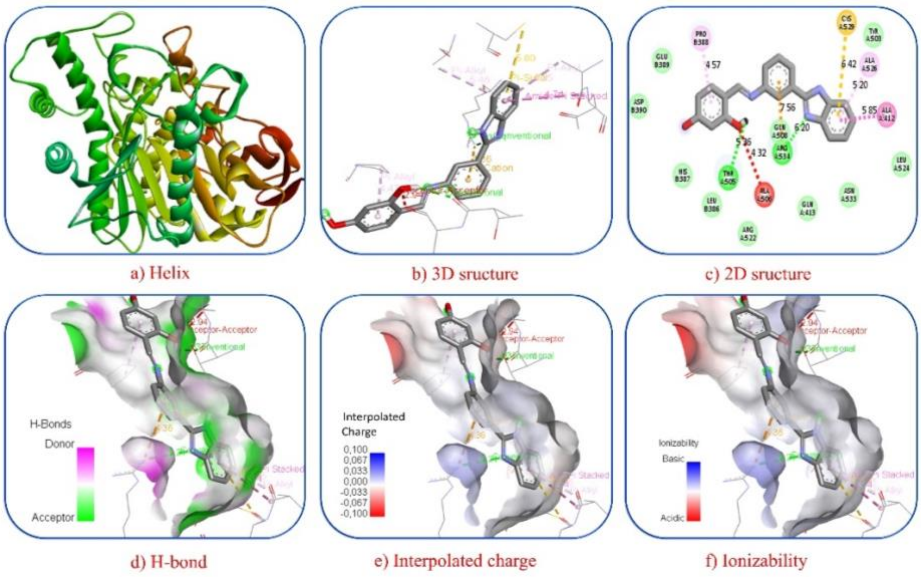

Figure 5. Molecular docking visual results of BIMSB compound with 4B84 enzyme.

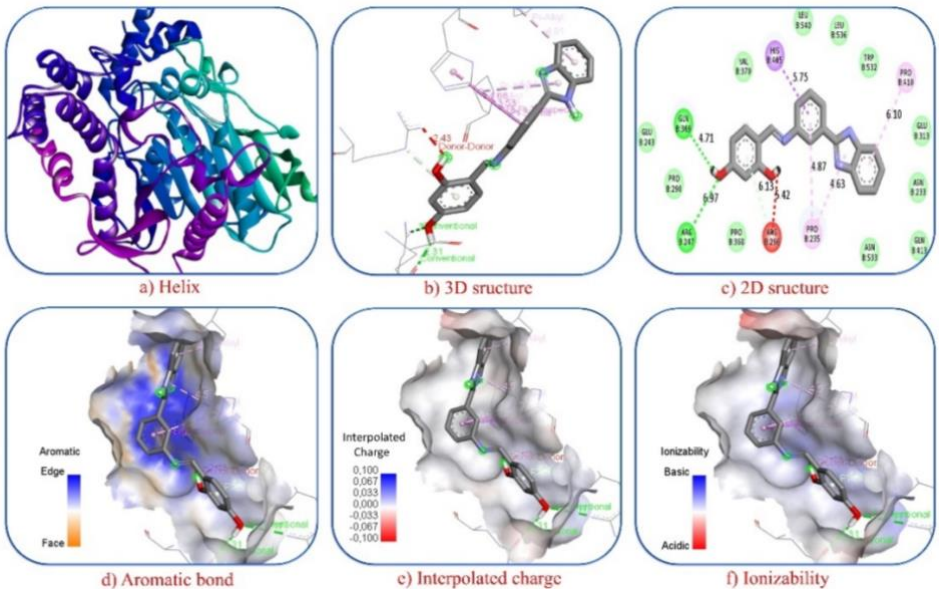

Figure 6. Molecular docking visual results of BIMSB compound with 4EY7 enzyme.

Table 7. The interaction parameters between BIMSB compound and 4B84, 4EY7 enzymes.

Type of Bond	Interacting Amino Acid (4B84)	Bond Length (Å)	Interacting Amino Acid (4EY7)	Bond Length (Å)
Van der Waals Interactions	GLU-389 ASP-390 HIS-387 ARG-522 GLN-413	-	GLU-243 PRO-290 ASN-533 GLN-413 TRP-532	-
Conventional H Bonds	THR-505 ARG-534	5.36 6.20	GLN-369 ARG-247	4.71 6.97
Unfavorable Acceptor-Acceptor	ALA-506	4.32	-	-
Pi-Cation	ARG-534	7.56	-	-
Pi-Sulfur	CYS-529	6.42	-	-
Amide-Pi Stacked	ALA-412	5.85	-	-
Pi–Alkyl	ALA-526 PRO-388	5.20 4.57	PRO-235 PRO-235 PRO-410	4.63 4.87 6.10
Unfavorable Donor-Donor	-	-	ARG-296	5.42
Pi-Sigma	-	-	ARG-296	6.13
Pi–Pi T-shaped	-	-	HIS-405	5.75

Figure 7 presents a two-dimensional visualization of the interactions of BIMSB with the enzymes PDB ID: 4B84 and 4EY7. The interaction types in the image are color-coded, and detailed classifications are provided for van der Waals, conventional hydrogen bonds, pi-alkyl, pi-sulfur, pi-cation, pi-sigma, pi–pi T-shaped, and other weak interactions. BIMSB formed hydrogen bonds and pi-cation/sulfur interactions with the 4B84 enzyme, particularly through residues such as ARG-534, THR-505, and CYS-529, while it formed both hydrogen bonds and weak interactions with the 4EY7

enzyme and amino acids such as GLN-369, ARG-247, and ARG-296. This structure clearly demonstrates that the compound forms versatile and strong bonds with target proteins.

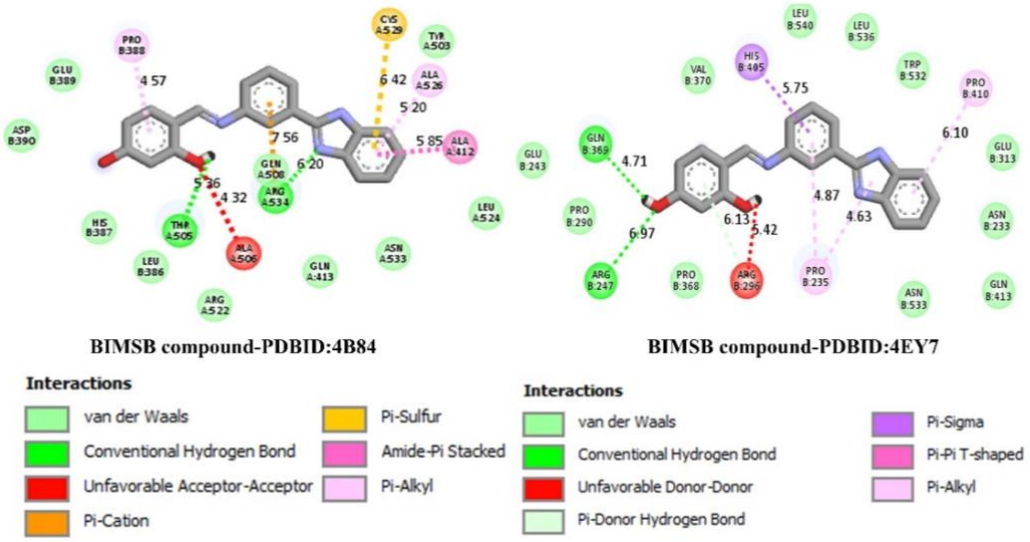

Figure 7. 2D Mode view of BIMSB Compound and PDBID: 4B84, PDBID: 4EY7 enzym.

3.8. ADMET Analysis

Computational ADMET modeling has become an increasingly important tool for predicting the pharmacokinetic and pharmacodynamic properties of new compounds at early stages in drug discovery and development (Anza et al., 2021; Qaddir et al., 2017). While this field has made significant progress, it continues to evolve to improve the predictive accuracy and comprehensiveness of in silico ADMET methods (Flores-Holguín et al., 2021; Samuel et al., 2021). Table 8 summarizes the pharmaceutically important physicochemical and lipophilic properties, as well as ADMET (Absorption, Distribution, Metabolism, Excretion, and Toxicity) parameters of BIMSB. The physicochemical properties of BIMSB (molecular weight, hydrogen bonding numbers, logP, and TPSA) conform to Lipinski's rules and theoretically support oral bioavailability. However, absorption parameters, particularly the human intestinal absorption (HIA) value of 0.009, were very low, indicating that the drug cannot be effectively absorbed when administered orally. While CaCo-2 permeability is relatively favorable, the extremely low HIA is a significant limitation for oral administration. In terms of distribution parameters, the low probability of BBB passage (0.083) suggests minimal central nervous system effects, although the moderate systemic distribution with a VD (0.87 L/kg) provides only a limited advantage. Regarding metabolism, the probability of CYP2D6 inhibition (0.929) was found to be quite high, posing a significant risk for potential drug-drug interactions. While low CYP3A4 inhibition provides an advantage, it does not compensate for the CYP2D6 risk. Elimination and half-life assessment, with a short T1/2 value of 0.71 hours,

indicates rapid elimination of the drug from the body, making the maintenance of therapeutic efficacy difficult. Toxicity parameters are a critical limiting factor for BIMSB: an Ames test result of 0.812 suggests high mutagenic potential, and an H-HT value of 0.34 indicates a moderate risk of hepatotoxicity. While low hERG inhibition and minimal acute oral toxicity are positive aspects, mutagenicity and liver toxicity raise potential safety concerns. ADMET data, particularly the very low oral absorption, short half-life, high CYP2D6 inhibition, and mutagenicity/hepatotoxicity risks, severely limit the potential of BIMSB as a strong drug candidate. These factors cannot be compensated for by theoretical pharmacochemical suitability or lipophilicity alone.

Table 8. BIMSB molecule's physicochemical and lipophilicity.

Property	BIMSB	Comment
Molecular Weight	329.12	Molecular Weight<500
nHA	5	Hydrogen bond acceptors<12
nHD	3	Hydrogen bond donors<7
logP	4.615	Log of the octanol/water partition coefficien: 0-5
TPSA	81.5	Topological Polar Surface Area:0-140
HIA	0.009	Category 1: HIA+(HIA<30%); Category 0: HIA-(HIA>=30%); The output value is the probability of being HIA+
Caco-2 Permeability	-5.037	Optimal: higher than -5.15 Log unit
BBB	0.083	The output value is the probability of being BBB+
VD	0.87	Volume Distribution Optimal: 0.04-20L/kg
CYP2D6	0.929	Category 1: Inhibitor; Category 0: Non-inhibitor; The output value is the probability of being inhibitor.
CYP3A4	0.21	Category 1: Inhibitor; Category 0: Non-inhibitor; The output value is the probability of being inhibitor.
$T_{1/2}$	0.71	The unit of predicted T1/2 is hours. ultra-short half-life drugs: 1/2<1 hour; short half-life drugs: T1/2 between 1-4 hours; intermediate short half-life drugs: T1/2 between 4-8 hours; long half-life drugs: T1/2>8 hours.
hERG Blockers	0.011	Category 1: active; Category 0: inactive; The output value is the probability of being active.
H-HT	0.34	Human Hepatotoxicity Category 1: H-HT positive(+); Category 0: H-HT negative(-); The output value is the probability of being toxic.
AMES Toxicity	0.812	Category 1: Ames positive(+); Category 0: Ames negative(-); The output value is the probability of being toxic.
Rat Oral Acute Toxicity	0.104	Category 0: low-toxicity; Category 1: high-toxicity; The output value is the probability of being highly toxic.

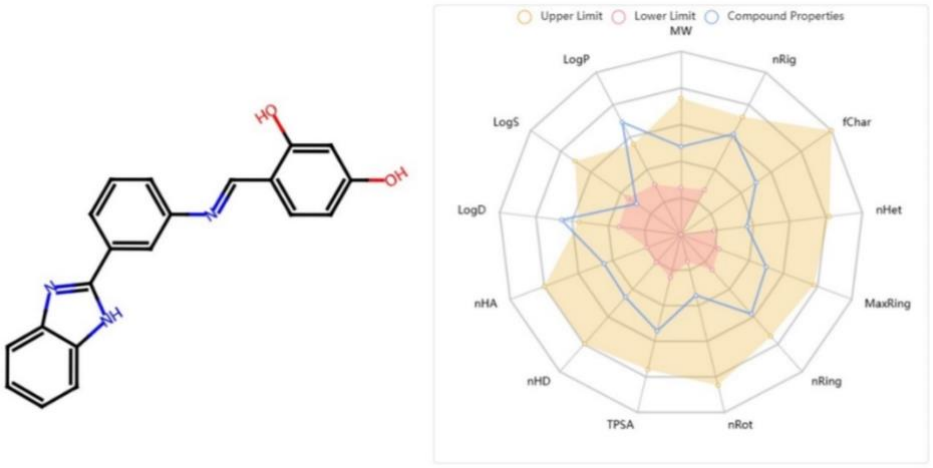

Figure 8. Color regions and physicochemical parameters of BIMSB molecule

4. Conclusion

In this study, the structural, electronic, nonlinear optical, and biological properties of the molecule (E)-4-(((3-(1*H*-benzo[d]imidazol-2-yl)phenyl)imino)methyl)benzene-1,3-diol (BIMSB) were investigated in detail using theoretical methods. BIMSB has a conjugated structure that combines benzoimidazole and dihydroxybenzene groups as a Schiff base, and this structure contributes to both the chemical stability and biological activity of the molecule. DFT-based B3LYP and B3PW91 calculations revealed that the optimized geometry of the molecule is stable and thermodynamically suitable. Molecular electrostatic potential (MEP) analyses identified regions with high reactivity, particularly in the benzene-1,3-diol and imino groups, and the HOMO–LUMO energy range provided important information about the chemical stability and reactivity of the molecule. NBO analysis demonstrated the contribution of hypercojugative interactions to the structural stability of the molecule, and Mulliken charge distribution allowed for the clear identification of electrophilic and nucleophilic centers. Calculated dipole moment, polarizability, and hyperpolarizability values indicate that the BIMSB molecule has significant potential in nonlinear optical (NLO) applications. Molecular docking studies revealed that BIMSB exhibits strong binding affinity with Alzheimer's disease (AD)-associated AChE enzymes (PDB: 4B84 and 4EY7), supporting the molecule's potential neuroprotective effect. Although the in silico ADMET profile of BIMSB theoretically possesses favorable physicochemical properties, it exhibits significant pharmacokinetic and toxicological limitations. Human intestinal absorption (HIA=0.009) is very low, severely restricting oral bioavailability. Furthermore, the high probability of CYP2D6 inhibition increases the risk of potential drug-drug interactions, while the high probability of Ames mutagenicity and moderate risk of hepatotoxicity negatively impact the safety profile. The short half-life ($T_{1/2}$=0.71 hours) also makes maintaining therapeutic levels difficult. These findings limit the direct evaluation of BIMSB as a

potent drug candidate with its current structure. Structural optimization of the molecule is necessary to improve its efficacy and safety. Therefore, the development of BIMSB should be supported by further studies primarily aimed at improving absorption, metabolic stability, and toxicity profiles.

Authors' Contributions

All authors contributed equally to the conception, design, implementation, analysis, and writing of the study.

Statement of Conflicts of Interest

There is no conflict of interest between the authors.

Statement of Research and Publication Ethics

The author declares that this study complies with Research and Publication Ethics.

References

Ahmad, I., Khan, H., & Serdaroğlu, G. (2023). Physicochemical properties, drug likeness, ADMET, DFT studies, and in vitro antioxidant activity of oxindole derivatives. *Computational biology and chemistry*, *104*, 107861.

Anza, M., Endale, M., Cardona, L., Cortes, D., Eswaramoorthy, R., Zueco, J., Rico, H., Trelis, M., & Abarca, B. (2021). Antimicrobial activity, in silico molecular docking, ADMET and DFT analysis of secondary metabolites from roots of three Ethiopian medicinal plants. *Advances and Applications in Bioinformatics and Chemistry*, 117–132.

Araújo, J. Q., Lima, J. A., Pinto, A. d. C., De Alencastro, R. B., & Albuquerque, M. G. (2011). Docking of the alkaloid geissospermine into acetylcholinesterase: a natural scaffold targeting the treatment of Alzheimer's disease. *Journal of Molecular Modeling*, *17*(6), 1401–1412.

Babu, P. D. S., Periandy, S., Mohan, S., Ramalingam, S., & Jayaprakash, B. (2011). Molecular structure and vibrational investigation of benzenesulfonic acid methyl ester using DFT (LSDA, B3LYP, B3PW91 and MPW1PW91) theory calculations. *Spectrochimica Acta Part A: Molecular and Biomolecular Spectroscopy*, *78*(1), 168–178.

Burley, S. K., Berman, H. M., Bhikadiya, C., Bi, C., Chen, L., Di Costanzo, L., Christie, C., Dalenberg, K., Duarte, J. M., & Dutta, S. (2019). RCSB Protein Data Bank: biological macromolecular structures enabling research and education in fundamental biology, biomedicine, biotechnology and energy. *Nucleic acids research*, *47*(D1), D464–D474.

Çimen, E., Gören, K., Tahiroğlu, V., & Yıldıko, Ü. (2025). The Theoretical Calculations by DFT Method and Analysis ADME, Molecular Docking of 1-(1-(4-hydroxybutyl)-6-methyl-4-phenyl-2-thioxohexahydropyrimidin-5-yl)ethan-1-one (pyrimidine-thiones) Compound [1-(1-(4-hidroksibütil)-6-metil-4-fenil-2-tioksoheksahidropirimidin-5-il)etan-1-on Bileşiğinin Moleküler Doking, ADME Analiz ve DFT Yöntemi ile Teorik Hesaplamalar]. *Osmaniye Korkut Ata Üniversitesi Fen Bilimleri Enstitüsü Dergisi*, *8*(3), 1129–1145. https://doi.org/10.47495/okufbed.1562370

El-Shamy, N. T., Alkaoud, A. M., Hussein, R. K., Ibrahim, M. A., Alhamzani, A. G., & Abou-Krisha, M. M. (2022). DFT, ADMET and Molecular Docking Investigations for the Antimicrobial Activity of 6, 6′-

Diamino-1, 1′, 3, 3′-tetramethyl-5, 5′-(4-chlorobenzylidene) bis [pyrimidine-2, 4 (1H, 3H)-dione]. *Molecules*, *27*(3), 620.

Farihi, A., Bouhrim, M., Chigr, F., Elbouzidi, A., Bencheikh, N., Zrouri, H., Nasr, F. A., Parvez, M. K., Alahdab, A., & Ahami, A. O. T. (2023). Exploring medicinal herbs' therapeutic potential and molecular docking analysis for compounds as potential inhibitors of human acetylcholinesterase in Alzheimer's disease treatment. *Medicina*, *59*(10), 1812.

Flores-Holguín, N., Frau, J., & Glossman-Mitnik, D. (2021). In silico pharmacokinetics, ADMET study and conceptual DFT analysis of two plant cyclopeptides isolated from rosaceae as a computational Peptidology approach. *Frontiers in Chemistry*, *9*, 708364.

G.W.T. M.J. Frisch, H. B. S., G.E. Scuseria, M.A. Robb, J.R. Cheeseman, G. Scalmani, V. Barone, B. Mennucci, G.A. Petersson, H. Nakatsuji, M. Caricato, X. Li, H.P. Hratchian, A.F. Izmaylov, J. Bloino, G. Zheng, J.L. Sonnenberg, M. Hada, M. Ehara, K. Toyota, R. Fukuda, J. Hasegawa, M. Ishida, T. Nakajima, Y. Honda, O. Kitao, H. Nakai, T. Vreven, J.A. Montgomery Jr., J.E. Peralta, F. Ogliaro, M. Bearpark, J.J. Heyd, E. Brothers, K.N. Kudin, V.N. Staroverov, R. Kobayashi, J. Normand, K. Raghavachari, A. Rendell, J.C. Burant, S.S. Iyengar, J. Tomasi, M. Cossi, N. Rega, J.M. Millam, M. Klene, J.E. Knox, J.B. Cross, V. Bakken, C. Adamo, J. Jaramillo, R. Gomperts, R.E. Stratmann, O. Yazyev, A.J. Austin, R. Cammi, C. Pomelli, J.W. Ochterski, R.L. Martin, K. Morokuma, V.G. Zakrzewski, G.A. Voth, P. Salvador, J.J. Dannenberg, S. Dapprich, A.D. Daniels, Ö. Farkas, J.B. Foresman, J.V. Ortiz, J. Cioslowski, D.J. Fox. (2009). *Gaussian 09*. In (Version Revision A.02)

Ganiev, B., Mardonov, U., & Kholikova, G. (2023). Molecular structure, HOMO-LUMO, MEP-–Analysis of triazine compounds using DFT (B3LYP) calculations. *Materials Today: Proceedings*.

Gören, K., Bağlan, M., Tahiroğlu, V., & Yıldıko, Ü. (2024). Theoretical Calculations and Molecular Docking Analysis of 4-(2-(4-Bromophenyl)Hydrazineylidene)-3,5-Diphenyl-4H-Pyrazole Molecule. *Journal of Advanced Research in Natural and Applied Sciences*, *10*(4), 786–802. https://doi.org/10.28979/jarnas.1516154

Gören, K., Bağlan, M., Tahiroğlu, V., & Yıldıko, Ü. (2025a). In-silico Drug Evaluation by Molecular Docking and ADME Studies, DFT Calculations of 2-(4-Chlorobenzyl)-6-(4-methoxyphenyl)imidazo [2,1-b][1,3,4]thiadiazole [2-(4-Klorobenzil)-6-(4-metoksifenil)imidazo[2,1-b][1,3,4]tiadiazol'un DFT Hesaplamaları, ADME Çalışmaları ve Moleküler Doking ile in-silico İlaç Değerlendirmesi]. *Bilecik Şeyh Edebali Üniversitesi Fen Bilimleri Dergisi*, *12*(2), 504–520. https://doi.org/10.35193/bseufbd.1632642

Gören, K., Bağlan, M., Tahiroğlu, V., & Yıldıko, Ü. (2025b). The Relationship Between AChE and BChE Enzymes and Alzheimer's Disease: ADME, Molecular Docking, and DFT Studies of Schiff Base-Substituted Phenylpyrimidine. *Celal Bayar University Journal of Science*, *21*(4), 1–15.

Gören, K., Bağlan, M., & Yıldıko, Ü. (2024a). Antimicrobial, and Antitubercular Evaluation with ADME and Molecular Docking Studies and DFT Calculatıons of (Z)-3-((1-(5-amino-1,3,4-thiadiazol-2-yl)-2-Phenylethyl)imino)-5-nitroindolin-2-one Schiff Base [(Z)-3-((1-(5-amino-1,3,4-tiadiazol-2-il)-2-feniletil)imino)-5-nitroindolin-2-on Schiff Bazının DFT Hesaplamaları ADME ve Moleküler Doking ile Antimikrobiyal ve Antitüberküloz Değerlendirmesi]. *Karadeniz Fen Bilimleri Dergisi*, *14*(4), 1694–1708. https://doi.org/10.31466/kfbd.1423367

Gören, K., Bağlan, M., & Yıldıko, Ü. (2024b). Melanoma Cancer Evaluation with ADME and Molecular Docking Analysis, DFT Calculations of (E)-methyl 3-(1-(4-methoxybenzyl)-2,3-dioxoindolin-5-yl)-acrylate Molecule. *Journal of the Institute of Science and Technology*, *14*(3), 1186–1199. https://doi.org/10.21597/jist.1467666

Gören, K., Bağlan, M., & Yıldıko, Ü. (2025). Analysis by DFT, ADME and Docking Studies of N'-(4-Hydroxy-3-Methoxybenzylidene)Naphtho[2,3-B]Furan-2-Carbohydrazide [Analysis by dft, adme and docking studies of n'-(4-hydroxy-3-methoxybenzylidene)naphtho[2,3-b]furan-2-carbohydrazide]. *Eskişehir Teknik Üniversitesi Bilim ve Teknoloji Dergisi B - Teorik Bilimler*, *13*(1), 7–23. https://doi.org/10.20290/estubtdb.1501639

Gören, K., & Yıldıko, Ü. (2024). Aldose Reductase Evaluation against Diabetic Complications Using ADME and Molecular Docking Studies and DFT Calculations of Spiroindoline Derivative Molecule [Spiroindolin Türevi Molekülünün DFT Hesaplamaları ve ADME ve Moleküler Doking Çalışmaları Kullanılarak Diyabetik Komplikasyonlara Karşı Aldoz Redüktaz Değerlendirmesi]. *Süleyman Demirel Üniversitesi Fen Bilimleri Enstitüsü Dergisi*, *28*(2), 281–292. https://doi.org/10.19113/sdufenbed.1474689

Gul, S., Jan, F., Alam, A., Shakoor, A., Khan, A., AlAsmari, A. F., Alasmari, F., Khan, M., & Bo, L. (2024). Synthesis, molecular docking and DFT analysis of novel bis-Schiff base derivatives with thiobarbituric acid for α-glucosidase inhibition assessment. *Scientific Reports*, *14*(1), 3419.

Jayaprakash, A., Arjunan, V., Jose, S. P., & Mohan, S. (2011). Vibrational and electronic investigations, thermodynamic parameters, HOMO and LUMO analysis on crotonaldehyde by ab initio and DFT methods. *Spectrochimica Acta Part A: Molecular and Biomolecular Spectroscopy*, *83*(1), 411–419.

Karabacak, M., Bilgili, S., & Atac, A. (2015). Molecular structure, spectroscopic characterization, HOMO and LUMO analysis of 3, 3′-diaminobenzidine with DFT quantum chemical calculations. *Spectrochimica Acta Part A: Molecular and Biomolecular Spectroscopy*, *150*, 83–93.

Khosravi, M., Murthy, V., & Mackinnon, I. D. (2020). Evaluation of DFT methods to calculate structure and partial atomic charges for zeolite N. *Computational Materials Science*, *171*, 109225.

Moustafa, H., Mohamed, G. G., & Elramly, S. (2020). Spectroscopic studies, Density Functional Theory calculations, and non-linear optical properties of binuclear Fe (III), Co (II), Ni (II), Cu (II), and Zn (II) complexes of OONN Schiff base ligand. *Journal of the Chinese Chemical Society*, *67*(10), 1783–1793.

Mushtaq, I., Ahmad, M., Saleem, M., & Ahmed, A. (2024). Pharmaceutical significance of Schiff bases: an overview. *Future Journal of Pharmaceutical Sciences*, *10*(1), 16. https://doi.org/10.1186/s43094-024-00594-5

Peitzika, S.-C., & Pontiki, E. (2023). A review on recent approaches on molecular docking studies of novel compounds targeting acetylcholinesterase in Alzheimer disease. *Molecules*, *28*(3), 1084.

Qaddir, I., Rasool, N., Hussain, W., & Mahmood, S. (2017). Computer-aided analysis of phytochemicals as potential dengue virus inhibitors based on molecular docking, ADMET and DFT studies. *Journal of vector borne diseases*, *54*(3), 255–262.

Release, S. (2019). 3: Maestro, Schrödinger, LLC: New York, NY, USA. 2019.

Sakr, M. A., Sherbiny, F. F., & El-Etrawy, A.-A. S. (2022). Hydrazone-based materials; DFT, TD-DFT, NBO analysis, fukui function, MESP analysis, and solar cell applications. *Journal of Fluorescence*, *32*(5), 1857–1871.

Salihović, M., Pazalja, M., Halilović, S. Š., Veljović, E., Mahmutović-Dizdarević, I., Roca, S., Novaković, I., & Trifunović, S. (2021). Synthesis, characterization, antimicrobial activity and DFT study of some novel Schiff bases. *Journal of Molecular Structure*, *1241*, 130670.

Samuel, Y., Garg, A., & Mulugeta, E. (2021). Synthesis, DFT analysis, and evaluation of antibacterial and antioxidant activities of sulfathiazole derivatives combined with in silico molecular docking and ADMET predictions. *Biochemistry Research International*, *2021*(1), 7534561.

Systèmes, D. (2016). Biovia, discovery studio modeling environment. *Dassault Systèmes Biovia: San Diego, CA, USA*.

Tahiroğlu, V., Gören, K., & Bağlan, M. (2025). In Silico drug evaluation by molecular docking, ADME studies and DFT calculations of 2-(6-chloro-2-(4-chlorophenyl)imidazo[1,2-a]pyridin-3-yl)-N, N-dipropylacetamide. *BMC Pharmacology and Toxicology*, *26*(1), 116. https://doi.org/10.1186/s40360-025-00958-4

Tahiroğlu, V., Gören, K., Bağlan, M., & Yıldıko, Ü. (2024). Molecular Docking and DFT Analysis of Thiazolidinone-Bis Schiff Base for anti-Cancer and anti-Urease Activity [Anti-Kanser ve Anti-Üreaz Aktivitesi için Tiazolidinon-Bis Schiff Bazının Moleküler Yerleştirme ve DFT Analizi]. *Journal of the Institute of Science and Technology*, *14*(2), 822–834. https://doi.org/10.21597/jist.1416223

Tahiroğlu, V., Gören, K., Çimen, E., & Yıldıko, Ü. (2024). Moleculer Docking and Theoretical Analysis of the (E)-5-((Z)-4-methylbenzylidene)-2-(((E)-4-methylbenzylidene)hydrazineylidene)-3-phenylthiazolidin-4-one Molecule. *Bitlis Eren Üniversitesi Fen Bilimleri Dergisi*, *13*(3), 659–672. https://doi.org/10.17798/bitlisfen.1471235

Tahiroğlu, V., Gören, K., Yıldıko, Ü., & Bağlan, M. (2024). IInvestigation, Structural Characterization and Evaluation of the Biological Potency by Molecular Docking of Amoxicillin Analogue of a Schiff Base Molecule. *International Journal of Chemistry and Technology*, *8*(2), 190–199. https://doi.org/10.32571/ijct.1410570